Detonation Mode and Frequency Variation Under High Loss Conditions

Scott I. Jackson[1], **Bok Jik Lee**[2], **and Joseph E. Shepherd**[3]
[1]Los Alamos National Laboratory, Los Alamos, NM 87545, USA
[2]King Abdullah University of Science and Technology, Thuwal 23955, SA
[3]GALCIT, California Institute of Technology, Pasadena, CA 91125, USA

1 Introduction

Detonation in tubing with diameters approaching the detonation reaction zone length has been shown to be capable of propagating at average velocities that are significantly below the Chapman-Jouguet (CJ) velocity that occurs in larger-diameter tubing. Prior work [2, 3] has shown a smooth decrease in average detonation velocity in small diameter tubing with decreasing pressure for stoichiometric propane-oxygen, reaching velocities as low as 0.5 D_{CJ}, where D_{CJ} is the Chapman-Jouguet detonation velocity, before the tube quenching limit was reached (Figure 1). This phenomenon has been the subject of considerable interest [1,4–7] for many decades. Investigation with a high-temporal-resolution framing camera diagnostic (discussed below) revealed that this velocity deficit was caused by the onset of a galloping detonation mode [3], which persisted over extremely long lengths of tubing with length-to-diameter ratios $L/d >$ 10,000.

Prior efforts have used microwave interferometry to obtain high-resolution detonation velocity histories to study near limit detonation [1, 4]. Lee *et. al.* [4] then processed these velocity histories to obtain histograms that qualitatively described six detonation modes as mixtures approached the failure limit. The galloping cycle in smooth tubes has been shown [7] to be approximately 350 non-dimensional tube lengths (L/d), while previous test facilities only had L/d values of 260 [4] and 645 [1]. Thus, observations of the full galloping cycle were limited and there was no opportunity to study its evolution.

In this work, we quantitatively analyze our prior experimental data [3] of galloping detonation with $L/d >$ 7,300 to characterize the sensitivity of this galloping mode to mixture initial pressure in small diameter tubing. Velocity-time profiles of galloping detonation are presented as a function of mixture pressure. Histograms are used to quantify the velocity probability at each test condition. These results are then interpolated to form a velocity probability map versus initial mixture pressure. A map of galloping frequency versus initial pressure is also reported.

2 Experiment

Detonations were propagated though small-diameter, transparent, polyurethane tubing filled with stoichiometric propane-oxygen mixtures of varying initial pressure. The tubing had an inner diameter of

Correspondence to: sjackson@lanl.gov

4.1-mm, a 30-m-long observation section, and was coiled in a spiral configuration with a radius varying from 0.2–0.5 m. A deflagration was initiated near the center of the spiral with a 30-mJ spark, which quickly transitioned to detonation. Three measurement stations that simultaneously measured pressure, ionization, and luminescence were spaced over the tubing length and allowed determination of the average combustion wave velocity. The initial mixture pressure was varied from 7 to 20 kPa, which yielded average detonation velocities between 0.57–0.94 D_{CJ} with good agreement across all diagnostics. Tests at 6.5 kPa were unable to initiate sustained combustion.

The chemiluminescence associated with combustion was also imaged with a high-speed framing camera (Vision Research Phantom) running at 12 kfps with a resolution of 256 px $\times$ 256 px. Comparison of the wave head in sequential images allowed determination of the interframe velocity. As the wave head motion was accurate to ± 1 pixel width (or 1.98 mm physical scale) and the interframe time was 83.3 μs, the measurement uncertainty associated with this analysis varied inversely with detonation velocity and was below $\pm 2.4\%$ for wave speeds above 1 km/s.

3 Results

The velocity histories for tests at initial pressures of 19.9, 12.0, 10.1, and 8.0 kPa are shown in Figures 2, 4, 6, and 8 respectively. At higher pressures, such as 19.9 kPa initial pressure (Figure 2), the detonation is seen to propagate in quasi-steady fashion near the CJ velocity, with small and intermittent velocity perturbations as shown in Figure 2. (Previous authors [4] have termed this propagation as a "stuttering" mode.) As the pressure is decreased, a galloping mode onsets and the wave velocity is seen to predominantly propagate near two distinct velocities near 0.4 D_{CJ} and 0.95 D_{CJ} as shown for the 12.0 kPa case (Figure 4), the 10.1 kPa case (Figure 6), and the 8.0 kPa case (Figure 8). These two velocities appear invariant throughout the galloping regime. The probability of the wave propagating near either velocity is a function of pressure, with decreasing pressure increasingly favoring the lower velocity and yielding a smooth decrease in the average wave velocity as seen in lower-resolution measurements (Figure 1).

As done previously for other mixtures [4], velocity histograms are used to quantify this effect. Figures 3, 5, 7, and 9 show histograms produced from binning the velocity in increments of 0.05 D_{CJ}, with the vertical axis representing the occurrence probability associated with each bin. The binning results confirm the qualitative observations from the velocity-time records. Distinct probability peaks are observed centered on 0.4 D_{CJ} and 0.95 D_{CJ} with the probability of the higher peak decreasing with decreasing pressure. Specifically, for only two bins centered on 0.4 D_{CJ} and 0.95 D_{CJ}, the ratio of low-to-high speed velocity occurrences is 1:99 for 19.9 kPa (Figure 2), 56:44 for 12.0 kPa (Figure 4), 67:33 for 10.1 kPa (Figure 6), and 73:27 for 8.0 kPa (Figure 8). We also note that characteristically similar bimodal distributions occur in the probability distributions of sine waves (without the asymmetry).

Performing a similar analysis on 10 tests fielded in this configuration allows interpolation to achieve a probability density function (PDF) for velocity as a function of pressure, as shown in Figures 10 (three-dimensional rendering) and 11 (two-dimensional plot). The PDF clearly shows that the 0.95 D_{CJ} velocity regime is almost exclusive from high pressures down to 15 kPa, after which it competes with the 0.4 D_{CJ} velocity regime. Above 12.5 kPa, the 0.95 D_{CJ} velocity regime is dominant. Below this value, the 0.4 D_{CJ} velocity regime has a higher probability. The 0.95 D_{CJ} velocity regime observed is indicative of a detonation. The 0.4 D_{CJ} velocity regime is characteristic of a shock wave trailed by a decoupled fast flame, which is generally the highest flame velocity observed before a local explosion transitions the deflagration mode to detonation. Thus, it may be that this experimental configuration has high enough wall losses to quench the detonation mechanism, while paradoxically having enough wall friction to promote rapid deflagration-to-detonation transition (DDT). Such a condition would preclude the occurrence of any stable deflagration or detonation mode.

The galloping frequency is also of interest. Power spectrums were taken of all velocity histories and interpolated to generate the map of frequency versus initial pressure shown in Figures 12 (three-dimensional rendering) and 13 (two-dimensional plot). The power of each frequency is seen to vary with each test, but a dominant frequency occurs near 1 kHz for all data below 15 kPa. Additional lower frequencies are present over initial pressures from 12–15 kPa at lower powers, but these oscillations do not persist as the initial pressure drops below 12 kPa. Thus, the frequency analysis indicates that galloping frequency does not appear to be a strong function of mixture pressure. Additional testing would be required to determine if it is a function of tube diameter or mixture kinetics. It is interesting that the average wave velocity drops with pressure while both the galloping frequency and peak velocities (0.4 D_{CJ} and 0.95 D_{CJ}) remain constant. This suggests that decreasing the pressure only affects the detonation quenching and deflagration (or DDT) acceleration process.

4 Conclusions

A quantitative analysis of the velocity distribution, velocity probability and galloping frequency versus initial pressure was performed for near-limit detonation propagation in stoichiometric propane-oxygen mixtures confined in polyethylene tubing with the tube diameter on the order of the detonation reaction zone length. The use of extremely long tube lengths (with $L/d >$ 7,300) allowed observation of over 15 galloping cycles. The results showed that two dominant velocity modes exist near 0.4 D_{CJ} and 0.95 D_{CJ}, with the lower velocity mode becoming more prevalent with decreasing mixture initial pressure. The results of multiple experiments were used to generate a PDF allowing visualization of this behavior. Analysis of the galloping frequency indicated that it was not a strong function of initial pressure.

References

[1] F. Haloua, M. Brouillette, V. Lienhart, and G. Dupre. Characteristics of unstable detonations near extinction limits. *Combustion and Flame*, 122:422–438, 2000.

[2] S.I. Jackson. *Gaseous Detonation Initiation via Wave Implosion*. PhD thesis, California Institute of Technology, Pasadena, CA, 2005.

[3] S.I. Jackson, B.J. Lee, W. Huang, F. Pintgen, J. Karnesky, Z. Liang, and J.E. Shepherd. Experimental detonation propagation under high loss conditions. In *Proceedings of the 22nd International Colloquium on the Dynamics of Explosions and Reactive Systems*, Minsk, Belarus, July 27–31 2009.

[4] J.J. Lee, G. Dupre, R. Knystautas, and L.H. Lee. Doppler interferometry study of unstable detonations. *Shock Waves*, 5(3):175–181, 1995.

[5] V.I. Manzhalei. Detonation of acetylene near the limit. *Combustion, Explosion, and Shock Waves*, 11(1):128–130, 1975.

[6] V.I. Manzhalei. Low-velocity detonation limits of gaseous mixtures. *Combustion, Explosion, and Shock Waves*, 35(3):296–302, 1999.

[7] H.D. Ng Y. Gao, J.H.S. Lee. Velocity fluctuation near the detonation limits. *Combustion and Flame*, 128(1-2):191–196, 2014.

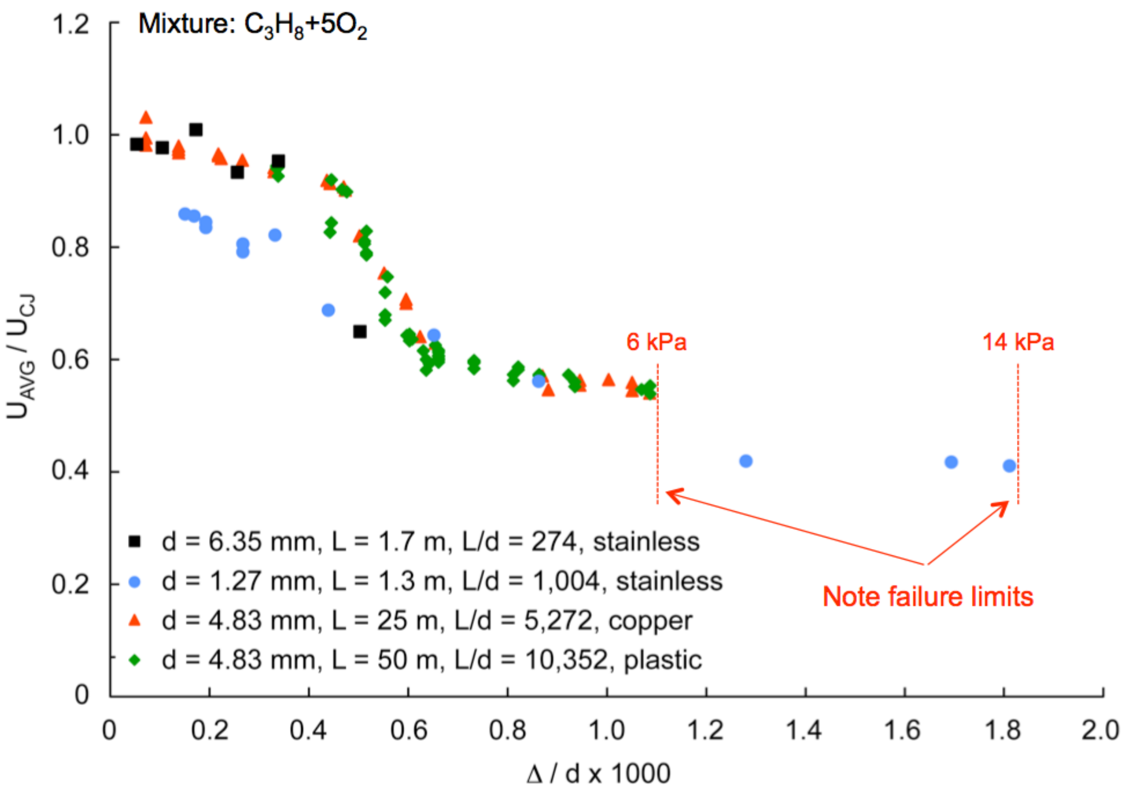

Figure 1: Data for C_3H_8+$5O_2$ in different tube diameters from Ref. 3. Parameter Δ is computed induction zone length and U is the wave velocity.

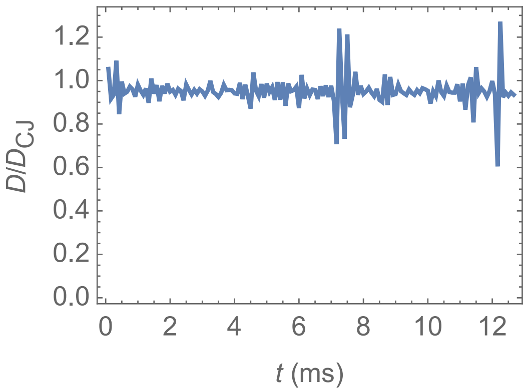

Figure 2: D vs. t at 19.9 kPa, D/D_{CJ}=0.95.

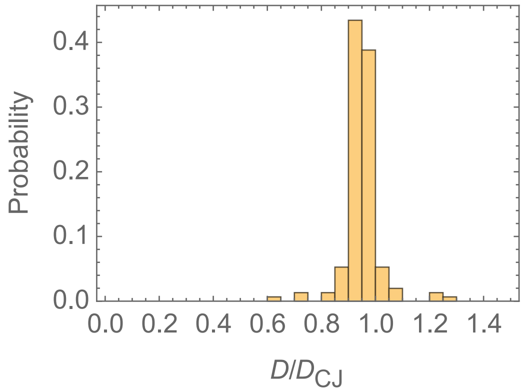

Figure 3: Velocity distribution at 19.9 kPa.

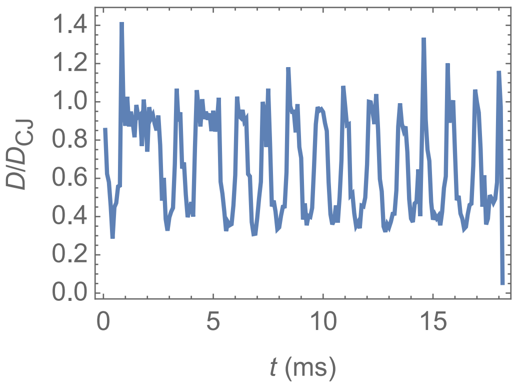

Figure 4: D vs. t at 12.0 kPa, D/D_{CJ}=0.67.

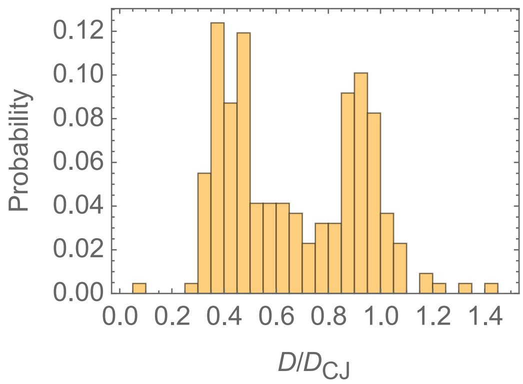

Figure 5: Velocity distribution at 12.0 kPa.

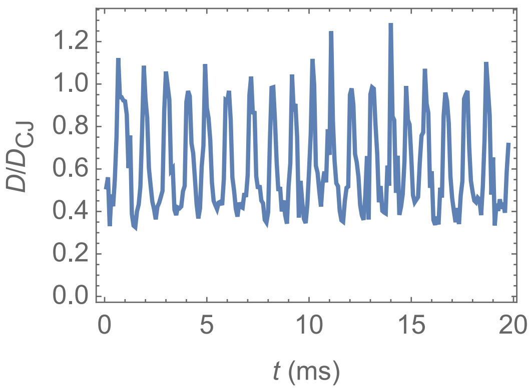

Figure 6: D vs. t at 10.1 kPa, D/D_{CJ}=0.62.

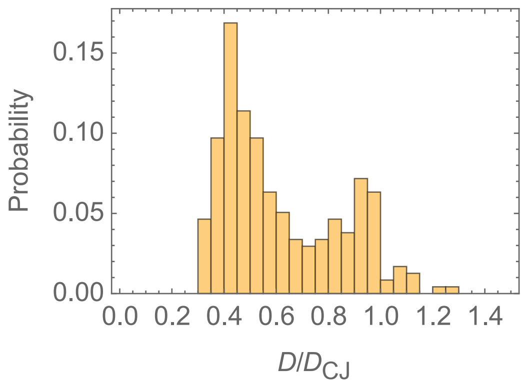

Figure 7: Velocity distribution at 10.1 kPa.

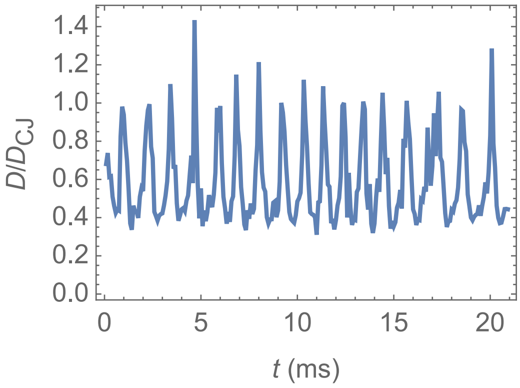

Figure 8: D vs. t at 8.0 kPa, D/D_{CJ}=0.58.

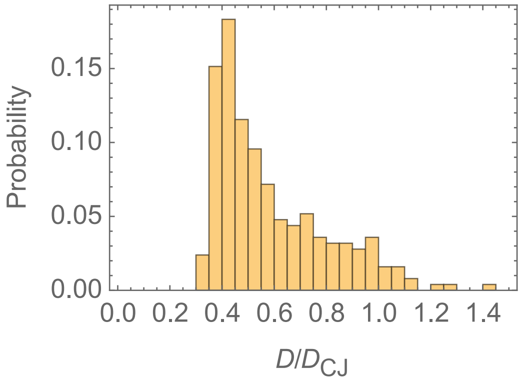

Figure 9: Velocity distribution at 8.0 kPa.

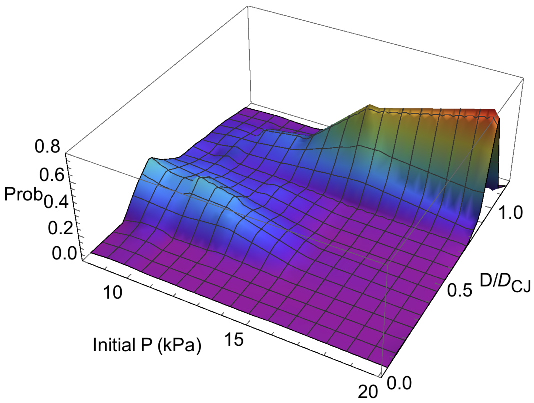

Figure 10: Perspective view of PDF for detonation velocity vs. pressure.

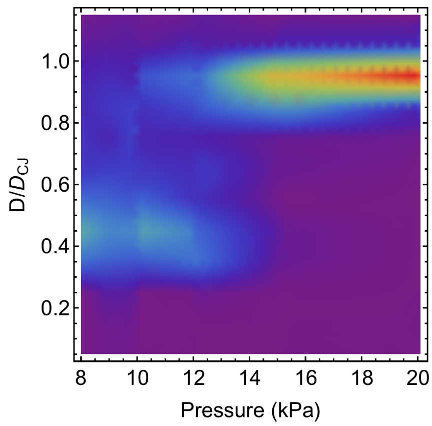

Figure 11: Top view of PDF for detonation velocity vs. pressure.

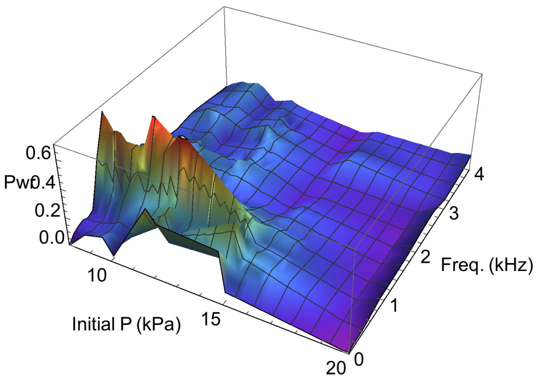

Figure 12: Perspective view of PDF for galloping frequency vs. pressure.

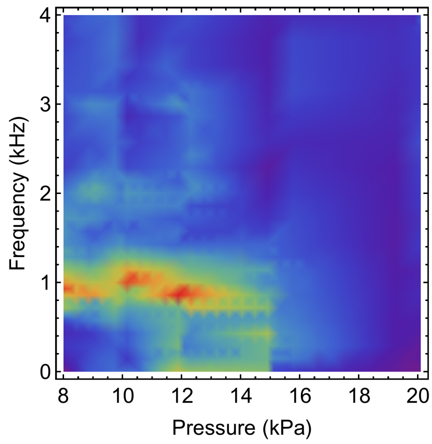

Figure 13: Top view of PDF for galloping frequency vs. pressure.